

Key to the Atlantic Gates of the Arctic

S. M. Gordeeva^{1,2,3}, T. V. Belonenko¹, and L. E. Morozova⁴

Received 29 December 2021; accepted 18 February 2022; published 4 May 2022.

We consider the decomposition of water temperature fields into the Empirical Orthogonal Functions (EOFs), also known as Principal Components (PCs). We use the GREP data (Global Reanalysis Ensemble Product) in this study and we examine water temperature at the horizon of 457 m for the period 1993–2019 in the area limited to 50°–80°N, 50°W–20°E. It is shown that the first two Principal Components of decomposition (PC1 and PC2) are responsible for 48% of the total variance, and all subsequent ones are smaller by an order of magnitude. The time series of PC1 and PC2 are further considered as indicators responsible for the transfer of Atlantic heat to the Arctic. Transport and heat fluxes have been calculated through the cross-section 64.5°N, which connects Iceland with Scandinavia. It is shown that PC1 characterizes transport through the cross-section, and PC2 is responsible for heat fluxes. The analysis of the spatial distribution of PC1 and PC2 loadings allowed us to introduce three new NAT, NAHT1, and NAHT2 indices determined by water temperature anomalies. The NAT index is responsible for the transport of Atlantic waters to the Arctic, and two identical indices NAT1 and NAT2 characterize the corresponding heat transfer by these waters. **KEYWORDS:** Atlantic Ocean; Arctic; AMOC; climate; transport; heat fluxes; empirical orthogonal functions; EOF; principal components; indicators; GREP.

Citation: Gordeeva, S. M., T. V. Belonenko, and L. E. Morozova (2022), Key to the Atlantic Gates of the Arctic, *Russ. J. Earth. Sci.*, 22, ES2004, doi:10.2205/2022ES000792.

1. Introduction

The Atlantic Ocean transports a quarter of the total oceanic and atmospheric heat from low latitudes to the Arctic [Buckley and Marshall, 2016]. The subpolar gyre in the North Atlantic modulates the European climate. Transport of Atlantic waters is one of the main factors that influenced the variability of the thermohaline struc-

ture of the Arctic [Beszczynska-Müller *et al.*, 2012; Pnyushkov *et al.*, 2018]. That is why the monitoring of the transferred water volume variability is extremely important for predicting large-scale climatic changes in the Northern Hemisphere. Heat is transferred to the Arctic using a system of currents called the Atlantic Meridional Overturning Circulation (AMOC). It is the AMOC that contributes (25%) to the maintenance of a temperate climate in North-Western Europe.

However, the AMOC has been an unprecedented slowdown over the past century. According to some models, this weakening by 2100 is 5–40% of the historical average state of a separate model, according to others – 15–60% for the same period. For all the scatter of these values, the trend leading to a constant weakening of the AMOC throughout the 21st century remains unchanged in all models [Cheng *et al.*, 2013]. This fact was noted as one of the ocean

¹Saint Petersburg State University, Saint Petersburg, Russia

²Russian State Hydrometeorological University, Saint Petersburg, Russia

³Shirshov Institute of Oceanology RAS, Moscow, Russia

⁴Saint Petersburg State University of Architecture and Civil Engineering, Saint Petersburg, Russia

keys in the special report of the Intergovernmental Panel on Climate Change [IPCC, 2019]. One of the reasons for the weakening of AMOC is the Gulf Stream, which carries warm waters from the tropics to the shores of Europe, and it is now weaker than at any time in the last millennium [Caesar et al., 2021]. Other reasons are associated with the weakening of convective processes in the region [Kuznetsova and Bashmachnikov, 2021].

The mechanism for maintaining the viability of AMOC is as follows: it is based on convection caused by differences in the density of seawater. Warm and salty Atlantic water moves from south to north, where it became cooler and, thus becoming denser and heavier, sinks into the depths of the ocean, where it returns to the south. However, current global warming disrupts this mechanism: an increase in precipitation and increased melting of the Greenland ice sheet add fresh water to the warm waters of the Gulf Stream, which reduces its salinity and, consequently, its density. In this case, less water sinks to a depth, and the recirculation flow of the AMOC is weakened. Further weakening of AMOC can be accompanied by natural disasters for many regions and countries: floods associated with the arrival of Atlantic storms on the continent, droughts, the spread of fires, abnormal temperatures in winter, and other extreme weather events associated with accelerating climate change [Grigorieva and Gulev, 2020; Volodin et al., 2008].

Calculations of meridional atmospheric heat and moisture transfers on various isobaric surfaces based on the ERA-Interim reanalysis data showed that the main influx of sensible and latent heat into the high-latitude Arctic in winter comes through the Atlantic part of its southern boundary at 70°N (from 0° to 80°E) in the layer from the surface up to 750 hPa [Alekseev et al., 2016]. As forecasts become reality, there is the necessity to identify individual characteristics of the climate system that can best characterize its variability and be considered as parameters for developing a forecast of the state of this system for a period of up to a decade. The North Atlantic is one of the most studied and well-documented regions of the World Ocean [Smith et al., 2010]. And in this case, the question arises: is it possible to find certain climate indices for monitoring the state of the system that characterizes the transfer of heat to the Arctic through the “Atlantic Gate”?

2. Previous Research on the Topic

This cross-section considers publications that discuss heat transport to the Arctic through the Atlantic Gate. Zhang [2008] provided an analysis of the first mode of the empirical orthogonal function (EOF1) for the observed average annual anomalies of the SSH (sea surface height) level altimetry and its relationship with the data on the subsurface temperature at 400 m in the extratropical North Atlantic for the period 1993–2003. It was found that the leading mode (EOF1) of the observed SSH anomalies has a dipole pattern, i.e. has the opposite sign between the subpolar gyre and the trajectory of the Gulf Stream. Such a dipole distribution of EOF1 is a hallmark of AMOC variability, and the ocean level is an integral characteristic containing information about the entire water column. Therefore, it is not surprising that the altimeter data in the study [Zhang, 2008] strongly correlate with the instrumental data on the temperature of the ocean layers in the North Atlantic. A stable relationship between altimetry measurements of the level and the water temperature was also revealed [Belonenko and Fedorov, 2018; Belonenko and Koldunov, 2019]. Zhang [2008] also noted a negative correlation between the subpolar circulation and the trajectory of the Gulf Stream. The main conclusion of the authors is as follows: the EOF1 shows the weakening of AMOC in the North Atlantic during the 1990s. However, this weakening is possibly part of a multi-month variation in variability, i.e. the authors do not exclude further strengthening of AMOC in the future. Continuing research in this direction, Yamamoto et al. [2020], Koul et al. [2020], and Biri and Klein [2019] indicate that possible changes in AMOC are a key source of uncertainty about future climate change. Moreover, temperature trend maps over the twentieth century show a prominent cooling region in the North Atlantic. Rahmstorf et al. [2015] presented evidence suggesting that this cooling is associated with a weakening of AMOC during the twentieth century and especially after 1970. Analyzing various AMOC indicators based on sea surface temperature, hemispheric temperature differences, indirect coral data, and ocean measurements, Rahmstorf et al. [2015] found that AMOC has partially recovered since 1990, but they also looked at the possible contribution of melt-

ing Greenland ice sheet to the slowdown in AMOC growth. AMOC characteristics are closely related to Atlantic multi-decadal variability and reflect its key elements [Zhang *et al.*, 2019]. Let us further consider how the AMOC can be numerically evaluated, what are its main parameters and what factors affect them.

2.1. AMOC Index

The AMOC index is usually associated with meridional transport at 26°N and is determined in sverdrups (1 Sv = 10⁶ m³/s):

$$Q(z) = \int_z^0 \int_{xw}^{xe} v(x, z') dx dz', \quad (1)$$

where Q is the zonal-integrated and total vertical meridional volumetric flow [Frajka-Williams *et al.*, 2019]. Here xw is the western border, xe is the eastern border of the region.

2.2. AMOC-Related Ocean Heat Transport

AMOC-related ocean heat transport in the North Atlantic across 26°N northward measured since 2004 [Bryden *et al.*, 2019]. Heat transfer is about 1.25 PW and exhibits large temporal variability over interannual timescales. On average, there was a 0.17 PW long-term decrease in ocean heat transfer over the year: from 1.32 PW before 2009 to 1.15 PW after 2009. A weakening of AMOC leads to cooling and a decrease in salinity in the upper ocean north of 26°N over the region from the Bahamas to Iceland. Cooling peaks were observed south of Iceland, where the surface sea temperature in 2016 was 2°C lower than in 2008. According to the estimates, the decrease in ocean heat transfer is due to a change in ocean heat content and 3/4 heat absorption by the atmosphere. Bryden *et al.* [2019] showed that the decrease in heat transfer and heat absorption by the atmosphere was precisely most evident in the path of the North Atlantic Current.

The warm water of subtropical origin in the Atlantic flows northward and carries heat to high latitudes. This poleward heat transfer is believed to be one of the possible reasons for the decrease in sea ice area and increase in ocean temperature

in the Arctic, but there are still no reliable estimates. Tsubouchi *et al.* [2020], using an inverse box model and measurements of volumetric transport over more than 20 years, showed that the average heat transport by the ocean was 305 ± 26 TW for 1993–2016. A significant heat transfer increase of 21 TW occurred after 2001, which is sufficient, the authors argue, to explain the accumulation of heat in the northern seas in recent years. Thus, ocean heat transfer may be one of the main drivers of climate change since the late 1990s. However, this increased heat transfer contrasts with the AMOC index at mid-latitudes and indicates the discontinuity of the AMOC measured at different latitudes in the Atlantic Ocean [Tsubouchi *et al.*, 2020].

Dong *et al.* [2021], based on altimetric and in situ data from the Atlantic Ocean since 1993, analyzed monthly mean temperature and salinity (T/S) profiles along zonal cross-sections both in the North Atlantic (26.5°N) and in the South Atlantic (20°S, 25°S, 30°S, and 35°S), which were then used to estimate meridional heat transfer. It turned out that these estimates strongly correlate with the AMOC index at all five latitudes, which is quite consistent with previous studies.

2.3. Influence of Buoyancy

Variations in AMOC caused by buoyancy are usually characterized by a low-frequency time scale, interhemispheric structure, cross-equatorial heat transfer, and links to the strength of the Northern Hemisphere and Gulf Stream gyres. The stronger AMOC is associated with the strengthening of gyres in the Northern Hemisphere, the Gulf Stream, and the transfer of heat by the ocean to the north throughout the basin. Larson *et al.* [2020] showed that low-frequency filtering of AMOC in the ocean-atmosphere model reproduces the buoyancy-driven AMOC model, but not the statistics of temporal variability. This analysis highlights the caveats to consider when choosing indices and filtering methods for estimating AMOC, which is also dependent on buoyancy.

2.4. Wind Influence

Loose *et al.* [2020] showed that winds along the eastern and northern boundaries of the Atlantic induce a basin-wide response of North Atlantic cir-

ulation and temperature. Due to these large-scale impacts, a single observation of temperature below the surface of the Irminger Sea indirectly provides information (up to 19%) about heat transfer across the entire Scotland-Iceland Ridge, far from the temperature observation point.

3. The Purpose and Formulation of the Research Problem

Thus, AMOC is the main engine of the global redistribution of heat and one of the main factors determining the warming in the Arctic. That is why AMOC in the North Atlantic is often called “The key of the Atlantic gateway to the Arctic”. Since this was established, the idea that AMOC variability could trigger irreversible climatic processes leading to collapse has remained on the agenda. The notion that AMOC can have more than one steady-state emerged in the 1980s as a powerful hypothesis to explain rapid climate variability. However, there is still uncertainty in the location of the stability thresholds relative to the current state of the climate, so today there is no reliable indication of exactly where the current AMOC is to the thresholds. In particular, *Weijer et al. [2019]* analyzed many studies related to the sustainability of AMOC and concluded that AMOC may be in or near equilibrium in the current climate. All this indicates that it is too early to put an end to the study of AMOC.

At the same time, AMOC is the main driver of climatic processes in the North Atlantic, and of the entire spectrum of characteristics influencing the warming of the Arctic, the most informative parameters are the water temperature and the corresponding heat fluxes transferred to the Arctic. The work aims to search for climatological indicators characterizing the transfer of heat from the Atlantic to the Arctic, which are correlated with the AMOC. All this indicates that it is too early to put an end to the study of AMOC.

4. Data and Processing Methods

For the analysis, we used the GREP data on water temperature and velocity components. GREP (Global Reanalysis Ensemble Product) is a reanalysis for the World Ocean, the data is available

on the Copernicus Marine Service (i.e. Copernicus Marine Environment Monitoring Service, <https://marine.copernicus.eu>). The product contains monthly averages of temperature, salinity, currents, and ice with a horizontal resolution of 1 degree for 75 vertical levels since 1993. The product is based on the synthesis of four oceanic reanalyses: GLORYS2V4 (Mercator Ocean, France), ORAS5 (ECMWF), GloSea5 (Meteorological Bureau, UK); and C-GLORS05 (CMCC, Italy), based on hydrodynamic models of the World Ocean. In all of them, satellite and field observations are jointly assimilated. This multi-model ensemble approach corrects uncertainties in the ocean state. The ensemble average can provide a more reliable estimate for certain regions and periods than each reanalysis product. The four reanalyses that form the basis for the GREP product cover the period 1993–2019, when altimetry data are available. GREP data are presented both in the form of four different time series and as unified ensemble series of monthly average data describing the ocean from surface to bottom (5900 m).

To calculate the EOF, we selected the water temperature values at the horizon of 457 m for the period from 1993 to 2019. within the boundaries of the region: 50°–80°N, 50°W–20°E on a 1° × 1° grid. Unlike most previous studies on this topic, we excluded from consideration the area south of 50°N. and, on the contrary, expanded the region in the north to include latitudes north up to 80°N. In the west and east, we excluded the Labrador and Barents Seas. We believe that this choice of the area borders is most consistent with the goal and objectives of the study. The choice of the horizon for analysis is driven by research [*Zhang, 2008*], which claims that the 400–500 m layer best reflects the attributes of Atlantic waters transported to the north. In addition, a comparison of several horizons showed that the chosen horizon is characterized by the greatest total variance of the first two principal components when decomposing fields into the empirical orthogonal functions (EOFs).

The initial processing of the GREP data included calculations of the average climatic annual cycle at each point of the grid averaged over the period 1993–2019 and anomalies of water temperature (AT) relative to the values of the annual course. The decomposition procedure into EOF was applied to these data.

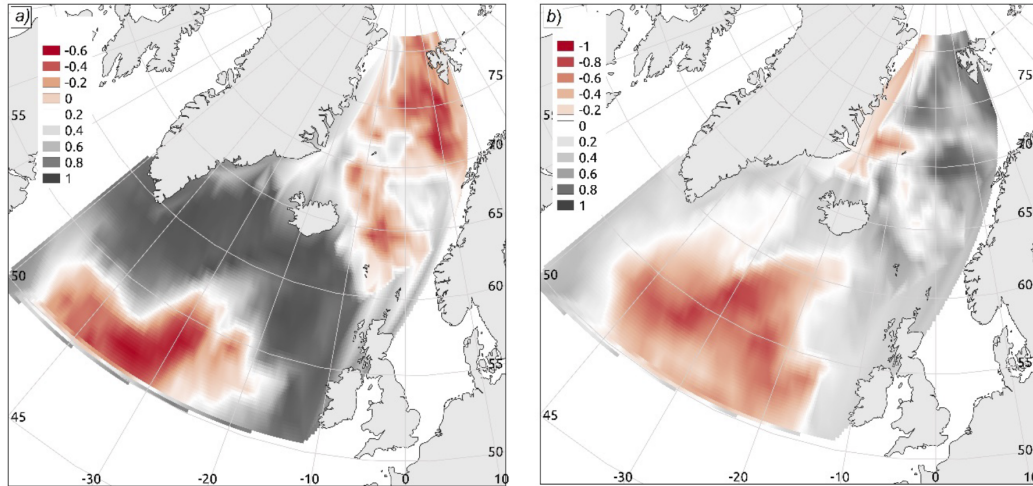


Figure 1. The distribution of PC1 (a) and PC2 (b) loadings of decomposition of water temperature anomalies in the North Atlantic.

Table 1. An Estimate of the Convergence of the Decomposition Into the Principal Components of the Water Temperature Anomaly Fields at the 457 m Horizon for the Period From 1993 to 2019

Decomposition characteristics	Principal component number									
	1	2	3	4	5	6	7	8	9	10
Eigenvalue	319.4	203.7	62.7	37.3	35.5	28.9	23.1	22.0	18.1	14.6
Described variance	0.29	0.19	0.06	0.04	0.03	0.02	0.02	0.02	0.02	0.01
Accumulated variance	0.29	0.48	0.54	0.58	0.61	0.63	0.65	0.67	0.69	0.70

5. Results

5.1. Decompositions Into Natural Orthogonal Functions

Figure 1 shows the decomposition of AT into EOFs (or principal components, PCs), and Table 1 shows an estimate of its convergence. Table 1 demonstrates that the first two components describe half of the total variance of the original fields: 29 and 19% (total 48%), respectively. The third and subsequent components determine an order of magnitude less variance, therefore, they will not be considered further. The identification of two principal components in the temporal variability of the AT fields at a horizon of 457 m indicates that on the layer under consideration there are two strong

modes in the water temperature fluctuations, reflecting two independent processes.

The spatial distribution of the principal component loadings (Figure 1) reflects the relationship between fluctuations in water temperature at points in the North Atlantic with the principal components. It can be seen that the first principal component (PC1) is associated with the variability of water temperature in a large area of the North Atlantic south of the North European Basin, including the Irminger Sea. The second principal component (PC2) characterizes the opposition of oscillations between the Greenland and Lofoten basins and the western periphery of the North Atlantic Current at latitudes 52°–60°N, i.e. defines the gradient of water temperature between the specified areas.

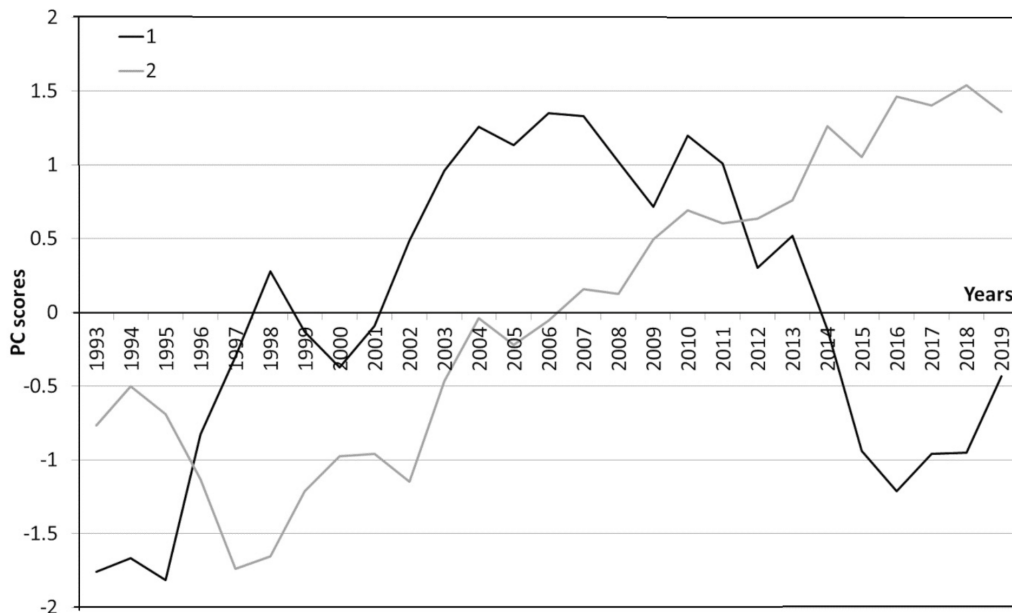


Figure 2. Temporal variability of PC1 (1) and PC2 (2) of decomposition of water temperature anomalies in the North Atlantic.

In the temporal variability of PC1 (Figure 2), several local trends reflecting the change in AT are well pronounced. It can be seen that from 1996 to 2007, the water temperature increased in the area located south of Iceland and the area “warmed up”, then, from 2007 to 2016, it “cooled down”, after which “heating” began again.

The temporal variability of PC2 has had a pronounced trend since 1998, determining a gradual weakening of the gradient between the basins North European Basin and western periphery North Atlantic Current. This means that the water temperature rises in cold areas, and on the contrary, it decreases in the warm areas of the western periphery North Atlantic Current.

5.2. AMOC Assessment: Transport Through the Vertical Cross-Section at 64.5°N

Figure 3 shows the assessment of the transport Q using the GREP data. For calculations, we chose a cross-section through 64.5°N, located north of the Faroe-Shetland Strait and connecting Iceland and the Scandinavian Peninsula. Integration according to formula (1) was carried out from the surface to the bottom. The average total transport Q is

3.22 Sv and it demonstrates the resulting northward flow while the transport in only one direction is 12.43 Sv from south to north and 9.21 Sv in the opposite direction. i.e. to the south. This means that transport through the cross-section in both directions is intensive and several times exceeds their total estimate. Figure 3 shows that the fluctuations in the total transport through the cross-section can be associated with the temporal variability of PC1. The significant warming south of Iceland, as discussed above in the period 2003–2012, can be associated with a weakening of the intensity of both northern and southern transport through the cross-section. Note transport to the north almost did not exceed the transport to the south in 2018–2019, as in 2007, so the total Q did not exceed 1 Sv although separately they were essential.

Figure 3 also shows trends using the parabolic functions. It can be seen that transport to the north, like transport to the south, increases by the end of the period under consideration. However, the flow directed to the south is more pronounced; therefore, for the total transport, there is a slight overall decrease with a linear trend coefficient of 0.034 Sv/year (Figure 3). We also obtained these estimates using a moving average (window width of 12 months) for data when seasonal variations were extracted.

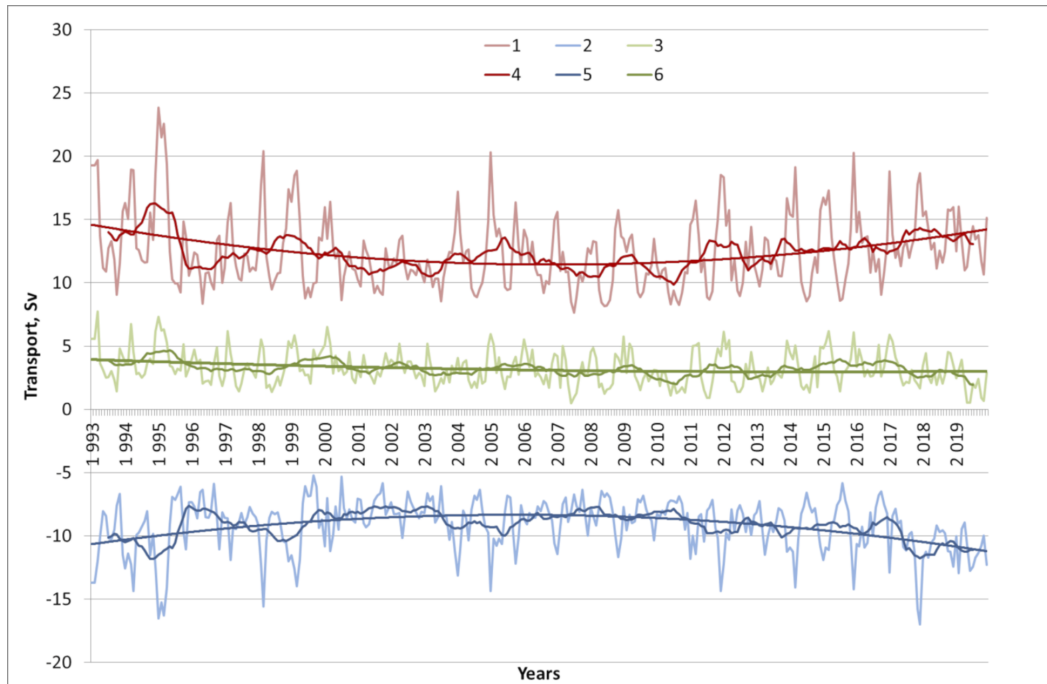


Figure 3. Temporal variability of the zonally integrated transports through the cross-section on 64.5°N (subtle lines) with 12-month moving average estimates (bold lines): northward (1, 4), southward (2, 5), and total (3, 6). Dark lines also indicate trends.

Figure 4 shows that the meridional transport Q is very heterogeneous in latitude. If in the western part of the cross-section up to 5°W the transport is directed mainly to the south, then in the eastern part, it sharply changes its direction and spreads to the north, reaching maximum values up to 6°E . This means that the main heat transfer to the Arctic is carried out mainly by the eastern branch of the North Atlantic Current, while in the western part of the cross-section, the transport is directed in the opposite direction.

5.3. Heat Fluxes Through the Cross-Section at 64.5°N

Figure 5 shows graphs of heat fluxes through the cross-section, and Figure 6 shows the average temperature through the cross-section. Note, although the average water temperature in the cross-section increases, the tendencies for heat fluxes remain the same as for flow rates: the total heat flux through the cross-section by the end of the considered period decreases. The linear trend in the growth of average temperature values is significant and is characterized by a coefficient of $0.0051^{\circ}\text{C}/\text{month}$.

However, this does not lead to an increase in the total heat fluxes through the cross-section due to the intensification of the southern flows through the strait.

5.4. Cross-Correlation of the Variability of the Principal Components, Values of Transport, and Heat Fluxes Through the Cross-Section at 64.5°N

To assess the statistical relationship of various parameters characterizing the transfer of heat through the cross-section, a cross-correlation matrix was constructed. For the calculations, the series was used, from which the seasonal variation was excluded using the moving average procedure with a window width of 12 months. The cross-correlation coefficients are presented in Table 2. It turned out that the average water temperature (T) in the vertical cross-section has a significant negative correlation coefficient (-0.792) with the heat flux to the south and slightly less (0.509) in the opposite direction. This means that the higher the temperature in the cross-section, the greater the heat flux to the south and north. However, in this

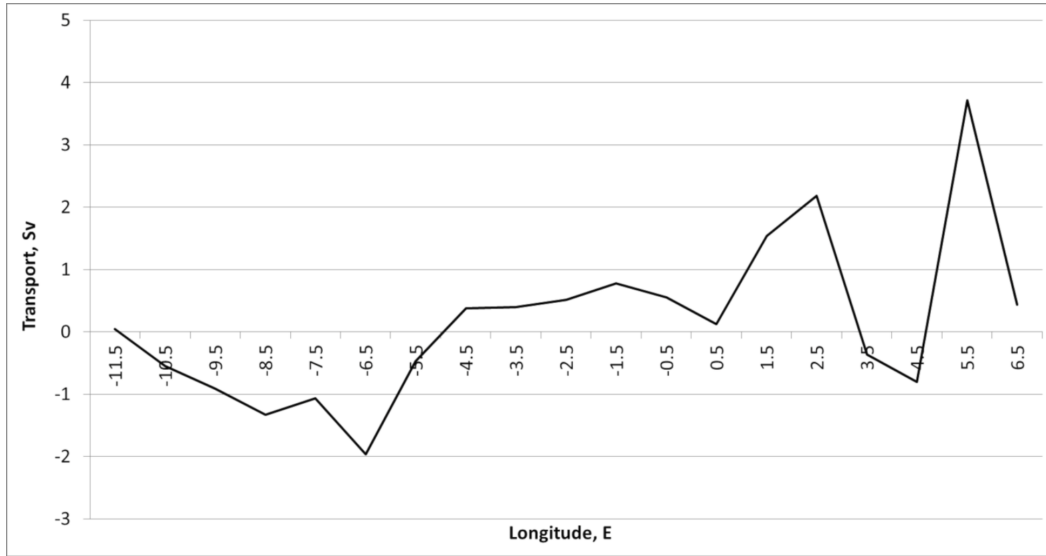


Figure 4. Zonal variability of the total transport Q through the cross-section on 64.5°N .

Table 2. Correlation Matrix of the Average Temperature on the Cross-Section Through 64.5°N , Heat Fluxes, Transports, and Principal Components

	T (temp.)	Total heat flux	Heat flow south	Heat flow north	Total transport	Transport to the north	Transport to the south
T (temp.)	1.000						
Total heat flux	-0.359	1.000					
Heat flow south	-0.792	0.471	1.000				
Heat flow north	0.509	0.391	-0.627	1.000			
Total transport	-0.446	0.731	0.311	0.321	1.000		
Transport to the north	-0.014	0.163	-0.359	0.518	0.568	1.000	
Transport to the south	-0.202	0.165	0.581	-0.461	-0.187	-0.915	1.000
PC1	0.120	0.121	0.243	-0.147	-0.528	-0.620	0.481
PC2	0.856	-0.260	-0.720	0.522	-0.259	0.118	-0.269

case, the correlation coefficient of the average temperature with the total flow transport is insignificant, since multidirectional flows neutralize this dependence. Also, there are no significant correlation coefficients of temperature with the estimates of flow transport, but at the same time, the total flow transport and heat flux are matched with a correlation coefficient of 0.731, as well as these characteristics in both directions (coefficients 0.518 – to the north and 0.581 – to the south). This relationship can be explained by the fact that the calculation of heat fluxes was based on estimates

that the higher the flow transport, the more heat is transferred by the flow in one direction or another. Note the significant correlation coefficient of -0.915 between the transport in both directions: this means that with an increase in the northward transport, the southward transport simultaneously decreases, which is physically explainable. A similar relationship is observed between heat fluxes in opposite directions (correlation coefficient -0.627): the greater the heat flux to the north, the less to the south. But at the same time, the total consumption and heat flux were matched with a correlation

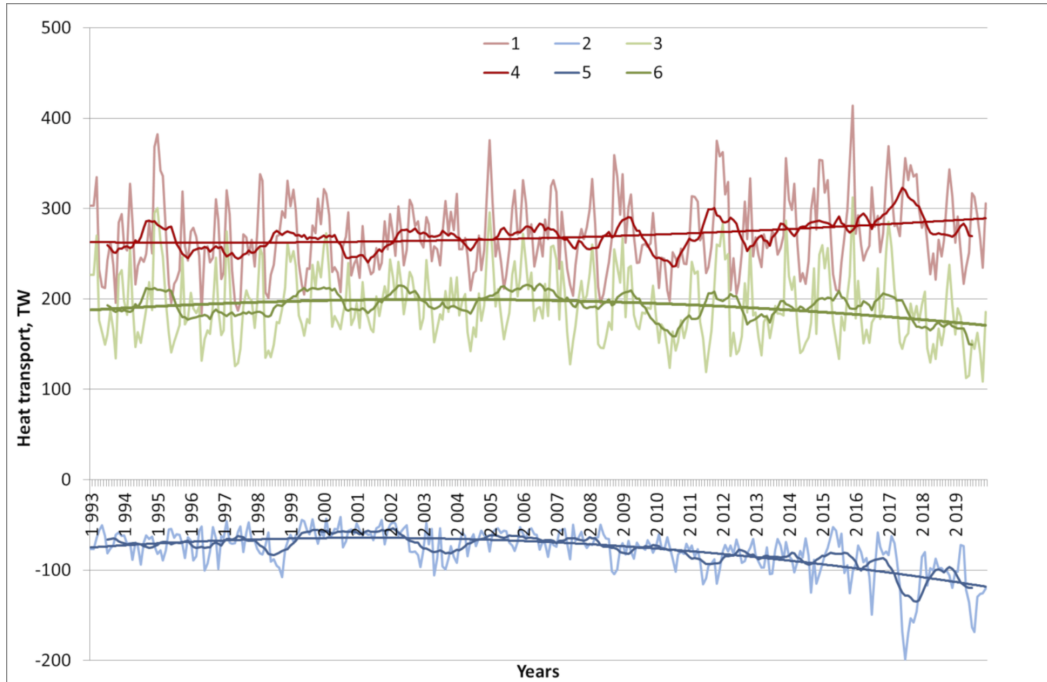


Figure 5. Temporal variability of the zonally integrated heat transports through the cross-section on 64.5°N (subtle lines) with 12-month moving average estimates (bold lines): northward (1, 4), southward (2, 5) and total (3, 6). Dark lines also indicate trends.

coefficient of 0.731, as well as these characteristics in both directions (coefficients 0.518 to the north and 0.581 to the south). Of greatest interest are the correlation coefficients of these characteristics with the principal components. PC1 and PC2 reflect different processes that determine the transfer of heat to the Arctic. If PC1 has a negative correlation with the total transport and also the transport to the north and thus is responsible for the volume of transport to the Arctic, then PC2 characterizes the temperature characteristics. The increase in the average water temperature in the cross-section is consistent (correlation coefficient 0.856) with PC2, as a result of which the heat fluxes to the north and south increase during the study period (0.522 and -0.720 , respectively).

Thus, the decomposition of the temperature fields on the EOF at the 457 m horizon allows us to consider PC1 as an indicator of flow transports. An increase in PC1 values also leads to a decrease in transport to the north. The decomposition component of PC2 is responsible for heat fluxes: an increase in PC2 by the end of the study period reflects warming in the cold North European Basin and cooling in a warm region south of Iceland,

which reduces the temperature gradient that determines PC2 between these regions. In what follows, we will consider PC1 as an indicator of the transport of the Atlantic Gates of the Arctic, and PC2 as an indicator of the corresponding heat fluxes.

5.5. Relationship Between PC1 and PC2 With Other Indices

Since we have defined above the role of PC1 and PC2 as climatic indices, it is necessary to understand how they can be related to other climatic indices, i.e. one should try to find the so-called “teleconnections” (see also [Bekryaev, 2019]). We examined the statistical relationship between PC1 and PC2 with 43 climatic indices (see <https://psl.noaa.gov/data/climateindices/>), including the AO (Arctic Oscillation), AMO (Atlantic multidecadal Oscillation), AMM (Atlantic Meridional Mode), NAO (North Atlantic Oscillation), etc. The series PC1 and PC2 were averaged to the annual average and cross-correlation was carried out for them with a shift of up to 5 years. Table 3 shows only those correlation coefficients (CC), the values of which

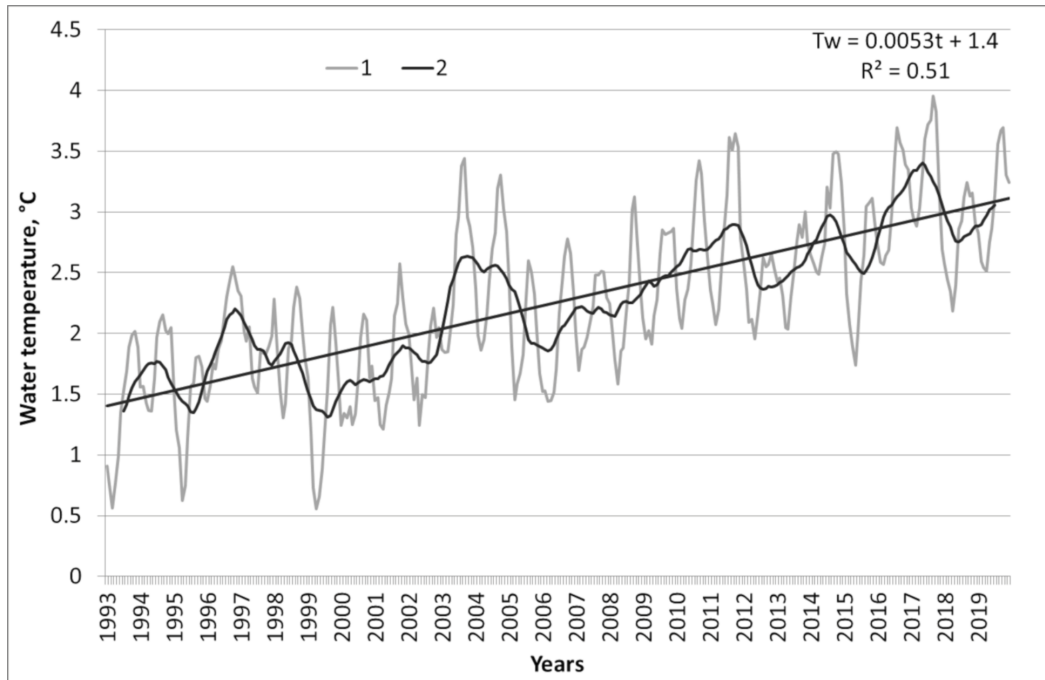


Figure 6. Zonally integrated mean water temperature (T_w) through the cross-section on 64.5°N (1) with 12-month moving average estimates (2). Dark lines also indicate trends.

exceed 0.6. In other cases, we believe that there is no relationship between climatic indices and principal components PC1 and PC2.

Table 3 shows the relationship between PC1 and the AMM (Atlantic Meridional Mode) index with a correlation coefficient of 0.61. The rationale for this index is given in [Chiang and Vimont, 2004]. This index is associated with the ten-year cycle of the Atlantic Ocean variability, the exact cause of which is still far from being established, despite the emergence of hydrodynamic models. AMM has traditionally been associated with ocean heat transport, although recent research has shown that atmospheric stochastic forcing is sufficient for this. Yamamoto et al. [2020] conducted a study based on hydrodynamic modeling, dividing the trend of water temperature variability over several decades into parts caused by surface heat flows and ocean dynamics. In the model, the horizontal advection of ocean heat primarily contributes to the heating of the upper layers of the subpolar Atlantic. However, if the vertical component is also considered, the dynamics of the ocean as a whole contribute to the cooling of the region. Northward heat flow is responsible for warming water temperatures in the subpolar North Atlantic, and it is the deepening of

Table 3. Cross-correlation coefficients with climate indices (<https://psl.noaa.gov/data/climateindices/list/>)

Index	CC	Shift
For PC1		
AMM	0.61	Synchronously
ACE Pacific	-0.71	3 years earlier
For PC2		
CAR	0.66	3 years earlier
Pacific warmpool	0.75	4 years earlier
Global Ta	0.87	5 years earlier
Global Ta	0.83	2 years later

the mixed layer depth that makes the ocean less susceptible to cooling, which also leads to relative warming by increasing the ocean’s heat capacity. Since both indicators PC1 and AMM belong to the same region and characterize the spatio-temporal variability of water temperature, the relationship between these characteristics occurs at a zero shift,

i.e. synchronously. the dynamics of the ocean as a whole contribute to the cooling of the region.

There is also a connection between PC1 and the index ACE Pacific (Eastern Pacific Accumulated Cyclone Intensities) with a correlation coefficient of -0.71 . This index characterizes the accumulated energy of cyclones and roughly corresponds to the wind energy generated by the tropical systems of the Pacific Ocean. Negative correlations with a shift of 3 years mean that a decrease in cyclonic activity in the tropical region of the Pacific Ocean is accompanied by an increase in PC1 in the North Atlantic and, accordingly, an increase in transport to the north through the 64.5°N cross-section after 3 years.

For the PC2, there is a connection with the indexes determined directly by temperature variability in different regions, in particular, with the CAR and Pacific Warmpool indices. The first index, CAR: Caribbean SST Index, is a time series of ocean surface anomalies averaged over the Caribbean region, and the second, Pacific Warmpool Region, is the same but for the Pacific Tropical Basin: 15°S – 15°N , 60°E – 170°E . Both indices show a significant relationship of them with PC2 and, consequently, with heat fluxes through the 64.5°N cross-section. There are the positive shifts 2 and 4 years which is understandable taking into consideration the geographical distances between the areas where these indicators were estimated.

And, finally, the connection between PC2 and the Global Ta index (Global Mean Land/Ocean Temperature), which characterizes the anomalies of the water surface of the World Ocean, and this relationship is noted both at positive and negative shifts ($+5$ and -2 years). The two-way relationship between PC2 and global temperature with high correlation coefficients reflects, first of all, the presence of a positive trend in both characteristics.

5.6. Indices of Atlantic Heat Transfer to the Arctic Based on Water Temperature Anomalies

Thus, the EOF method applied to the water temperature distribution fields revealed two main modes of its variability, characterizing about half of the total variance, determining their spatial patterns, and the interannual structure of fluctuations. Meanwhile, the principal components are used pri-

marily to identify areas of manifestation of these main modes of variability. At the same time, the construction of the principal components requires specific calculations and certain skills of their analysis. Therefore, instead of PC1 and PC2, we can use the characteristic itself (in this case, temperature anomalies AT) at points where the loadings are maximum. We can say that we apply here an approach similar to that of *Hurrell et al.* [2003], where, instead of PC1 built atmospheric pressure distributions, the NAO index is considered as the difference between the standardized atmospheric pressure anomalies between the Azores and Iceland. In our case, the analog of PC1 is AT in the coordinates 59° – 61°N , 28° – 30°W (in this area PC1 loading 0.95, see Figure 1a). The corresponding time series AT will be called the NAT index, which characterizes the North Atlantic Transport to the north through a section of 64.5°N .

For PC2, which characterizes the heat transfer through the cross-section, we set the indices of the North Atlantic Heat Transport – NAHT1 or NAHT2 built using the temperature anomalies of water on the horizon 457 m in two areas (see Figure 1b):

- 68° – 69°N , 1° – 2°E (PC2 loading $+0.89$)
- NAHT1,
- 56° – 57°N , 30° – 31°W (PC2 loading -0.85)
- NAHT2.

Thus, we are introducing three new indices: NAT, NAHT1, and NAHT2 (Figure 7), which are responsible for the transport of Atlantic waters and the corresponding transfer of Atlantic heat to the Arctic. Currently, the length of the rows NAT, NAHT1, and NAHT2, constructed according to GREP data, is 324 values. The time series responsible for heat transfer to the Arctic [*Gordeeva and Belonenko, 2022*] in text format are available at the website of Earth Science Data Base (ESDB) repository [<http://esdb.wdcb.ru/>] located in Geophysical Center RAS.

6. Discussion and Conclusions

Above, we examined the decomposition of water temperature fields at a horizon of 457 m on the EOF in the selected area: 50° – 80°N , 50°W – 20°E . The choice of the region and horizon for decomposition is justified. We also justified the choice of a zonal cross-section through 64.5°N , connecting

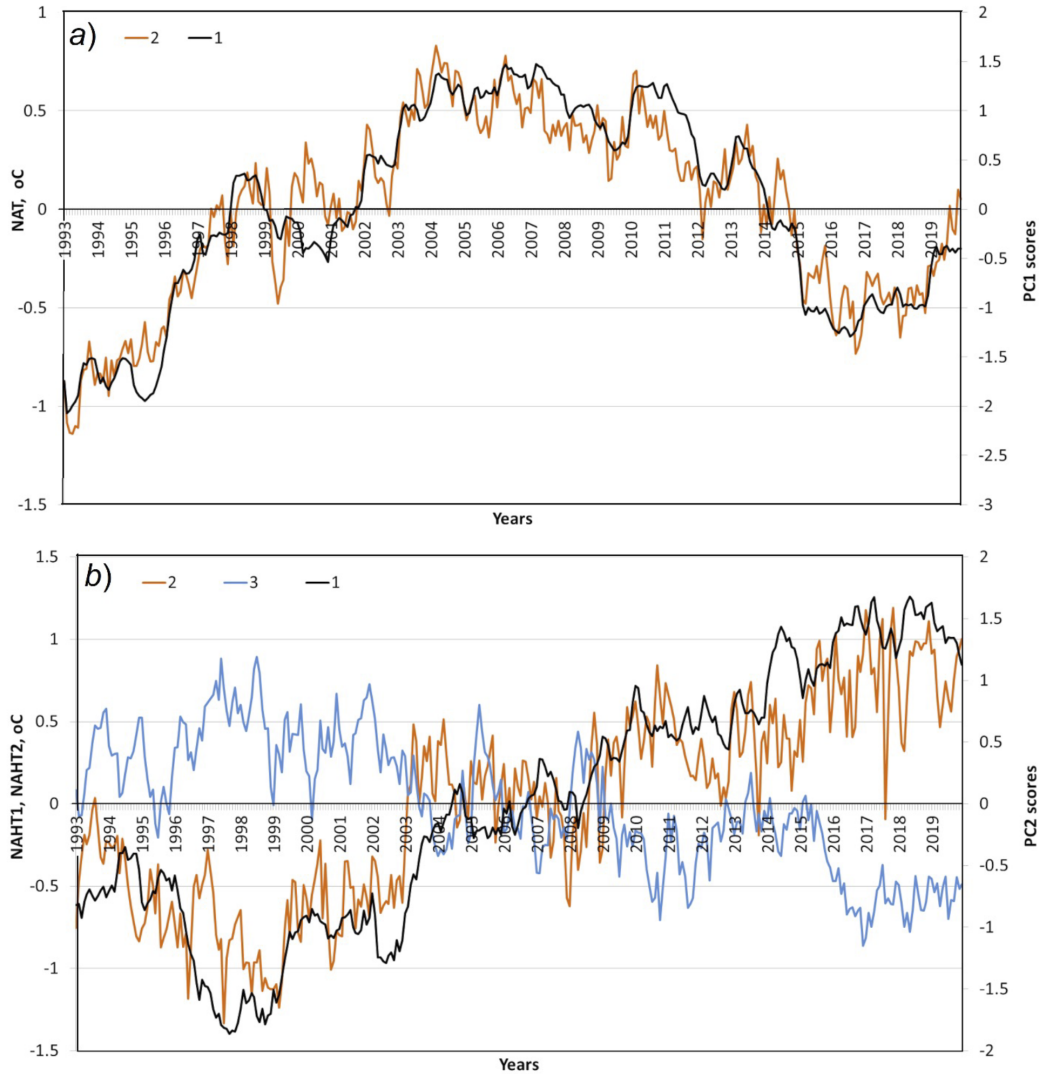


Figure 7. Temporal variability of (a): PC1 (line 1) and NAT (line 2); (b): PC2 (line 1), NAHT1 (line 2), and NAHT2 (line 3).

Iceland with Scandinavia, through which we calculated flow transport and heat fluxes.

We found that 48% of the variance falls on the first two principal components of the EOF decomposition, and all subsequent components contribute an order of magnitude less than the first two, which made it possible to limit the number of considered components to the first two. We also found that PC1 and PC2 characterize different processes. If PC1 has a significant negative correlation with the total and northward flow transports, then, therefore, it is responsible for the volume of transport to the Arctic. PC2 is directly responsible for heat transfer through the cross-section. These circumstances make it possible to consider the time series

PC1 and PC2 of the decomposition of temperature fields in the region of 50°–80°N, 50°W–20°E as quantitative indicators characterizing the transport and transfer of heat to the Arctic from the Atlantic Ocean. This explains the somewhat ambitious title of our article but reflects the actual state of things.

Climate change has a significant impact on the state of the region and is also associated with complex relationships with processes taking place in other parts of the planet. Therefore, it is so important to find indicators that can be used to track (monitor) climate changes in the region and reflect the impact of these changes on the environment. We believe that the analysis performed allows us

to consider in this vein the PC1 and PC2 indices calculated by us. In contrast to the many other indexes like AMO/AMV (Atlantic Multi-Decade Oscillation/Variability) indices [*Yamamoto et al., 2020*], as well as SPG (subpolar gyre - variability in the North Atlantic Subpolar Gyre), or NASPG (The North Atlantic subpolar gyre) [*Biri and Klein, 2019*], characterizing the variability of the North Atlantic Subpolar Gyre, or ENA (the eastern subpolar North Atlantic) [*Koul et al., 2020*], which are limited by the latitude 60°N, we consider a more northern region up to 80°N, which allows us to more accurately respond to the task of transferring heat to the Arctic through the Atlantic Gate. The PC1 and PC2 indices developed by us have a simple physical substantiation and can serve for monitoring climatic changes in the region.

Analysis of the spatial distributions of PC1 and PC2 allowed us to identify areas (points) in which the temporal variability of AT correlates with PC1 and PC2 with coefficients of 0.85–0.95. This makes it possible to introduce into consideration the NAT, NAHT1, and NAHT2 indices responsible for the transport of Atlantic waters and the corresponding heat transfer to the north. They can be easily calculated and can serve as a basis for monitoring climate processes in the region instead of PC1 and PC2.

Along the way, we have also shown that climatic processes in the region are interdependent with other processes occurring many thousands of kilometers away. This approach made it possible to detect the so-called “teleconnection”, in particular, with cyclonic activity and heat anomalies in the tropical Pacific Ocean, as well as with water surface temperature anomalies in the Caribbean Sea. It is important to note that PC1, which is responsible for the transport of water through the cross-section, correlates with the “dynamic” indices: the AMM index, which is responsible for the variability of circulation in the Atlantic, and the ACE Pacific index, which reflects the intensity of cyclonic activity in the tropical zone of the Pacific Ocean. At the same time, PC2, which reflects the variability of heat fluxes through the cross-section, correlates with CAR, Pacific Warmpool, and Global Ta, which are responsible for the variability in surface temperature distributions in the World Ocean.

Acknowledgments. The publication was funded by Saint Petersburg State University, project No 93016972.

References

- Alekseev, G. V., S. I. Kuzmina, et al. (2016), Impact of atmospheric heat and moisture on Arctic warming in winter, *Fundamental and Applied Climatology*, 1, 43–63, (In Russian) [Crossref](#)
- Belonenko, T. V., A. M. Fedorov (2018), Steric Level Fluctuations and Deep Convection in the Labrador and Irminger Seas, *Izvestiya, Atmospheric and Oceanic Physics*, 54, No. 9, 1039–1049, [Crossref](#)
- Belonenko, T. V., A. V. Koldunov (2019), Trends of Steric Sea Level Oscillations in the North Atlantic, *Izvestiya, Atmospheric and Oceanic Physics*, 55, No. 9, 1106–1113, [Crossref](#)
- Beszczynska-Müller, A., E. Fahrbach, et al. (2012), Variability in Atlantic water temperature and transport at the entrance to the Arctic Ocean, 1997–2010, *ICES Journal of Marine Science*, 69, No. 5, 852–863, [Crossref](#)
- Biri, S., B. Klein (2019), North atlantic subpolar gyre climate index: A new approach, *Journal of Geophysical Research: Oceans*, 124, 4222–4237, [Crossref](#)
- Bryden, H. L., W. E. Johns, et al. (2019), Reduction in ocean heat transport at 26°N since 2008 cools the eastern subpolar gyre of the North Atlantic Ocean, *Journal of Climate*, [Crossref](#)
- Bekryaev, R. V. (2019), Interrelationships of the North Atlantic multidecadal climate variability characteristics, *Russ. J. Earth Sci.*, 19, ES3004, [Crossref](#)
- Buckley, M. W., J. Marshall (2016), Observations, inferences, and mechanisms of the Atlantic Meridional Overturning Circulation: A review, *Reviews of Geophysics*, 54, No. 1, 5–63, [Crossref](#)
- Caesar, L., G. D. McCarthy, et al. (2021), Current Atlantic Meridional Overturning Circulation weakest in last millennium, *Nature Geoscience*, 14, No. 3, 118–120, [Crossref](#)
- Cheng, W., J. C. H. Chiang, D. Zhang (2013), Atlantic Meridional Overturning Circulation (AMOC) in CMIP5 Models: RCP and Historical Simulations, *Journal of Climate*, 26, No. 18, 7187–7197, [Crossref](#)
- Chiang, J. C. H., D. J. Vimont (2004), Analogous meridional modes of atmosphere-ocean variability in the tropical Pacific and tropical Atlantic, *Journal of Climate*, 17, No. 21, 4143–4158, [Crossref](#)
- Dong, S., G. Goni, et al. (2021), Synergy of in situ and satellite ocean observations in determining meridional heat transport in the Atlantic Ocean, *Journal of Geophysical Research: Oceans*, 126, e2020JC017073, [Crossref](#)
- Frajka-Williams, E., I. J. Ansorge, et al. (2019), Atlantic Meridional Overturning Circulation: Observed Transport and Variability, *Frontiers in Marine Science*, 6, [Crossref](#)
- Gordeeva, S. M., T. V. Belonenko (2022), New indicators responsible for heat transfer from the Atlantic to the Arctic, *ESDB repository, GCRAS*, [Crossref](#)

- Grigorieva, V., S. K. Gulev (2020), Wave climate in subarctic seas from Voluntary Observing Ships: 1900–2020, *Russ. J. Earth. Sci.*, 20, ES14015, [Crossref](#)
- Hurrell, J. W., et al. (2003), The North Atlantic Oscillation: Climate Significance and Environmental Impact, *Geophysical Monograph*, 134 American Geophysical Union, US. [Crossref](#)
- IPCC 2019 (2019), *Climate Change and Land: an IPCC special report on climate change, desertification, land degradation, sustainable land management, food security, and greenhouse gas fluxes in terrestrial ecosystems*, 874 pp. IPCC, Switzerland. (<https://www.ipcc.ch/site/assets/uploads/2019/11/SRCCL-Full-Report-Compiled-191128.pdf>)
- Koul, V., J.-E. Tesda, et al. (2020), Unraveling the choice of the north Atlantic subpolar gyre index, *Scientific Reports*, 10, 1005, [Crossref](#)
- Kuznetsova, D. A., I. L. Bashmachnikov (2021), On the Mechanisms of Variability of the Atlantic Meridional Overturning Circulation (AMOC), *Oceanology*, 61, No. 6, 843–855, [Crossref](#)
- Larson, S. M., M. W. Buckley, A. C. Clement (2020), Extracting the Buoyancy-Driven Atlantic Meridional Overturning Circulation, *Journal of Climate*, 33, 4697–4714, [Crossref](#)
- Loose, N., P. Heimbach, et al. (2020), Quantifying dynamical proxy potential through shared adjustment physics in the North Atlantic, *Journal of Geophysical Research: Oceans*, 125, e2020JC016112, [Crossref](#)
- Pnyushkov, A. V., I. V. Polyakov, et al. (2018), Heat, salt, and volume transports in the eastern Eurasian Basin of the Arctic Ocean from 2 years of mooring observations, *Ocean Sci.*, 14, No. 6, 1349–1371, [Crossref](#)
- Rahmstorf, S., J. E. Box, et al. (2015), Exceptional twentieth-century slowdown in Atlantic Ocean overturning circulation, *Nature Climate Change*, 5, No. 5, 475–480, [Crossref](#)
- Smith, G. C., K. Haines, et al. (2010), Impact of hydrographic data assimilation on the modelled Atlantic meridional overturning circulation, *Ocean Sci.*, 6, 761–774, [Crossref](#)
- Tsubouchi, T., K. Våge, et al. (2020), Increased ocean heat transport into the Nordic Seas and Arctic Ocean over the period 1993–2016, *Nature Climate Change*, [Crossref](#)
- Volodin, E. M., V. Ya. Galin, et al. (2008), Mathematical modeling of potential catastrophic climate changes, *Russ. J. Earth Sci.*, 10, ES2004, [Crossref](#)
- Weijer, W., W. Cheng, et al. (2019), Stability of the Atlantic Meridional Overturning Circulation: A Review and Synthesis, *Journal of Geophysical Research: Oceans*, [Crossref](#)
- Yamamoto, A., H. Tatebe, M. Nonaka (2020), On the emergence of the Atlantic multidecadal SST signal: A key role of the mixed layer depth variability driven by North Atlantic Oscillation, *Journal of Climate*, [Crossref](#)
- Zhang, R. (2008), Coherent surface-subsurface fingerprint of the Atlantic meridional overturning circulation, *Geophysical Research Letters*, 35, No. 20, [Crossref](#)
- Zhang, R., R. Sutton, et al. (2019), A Review of the Role of the Atlantic Meridional Overturning Circulation in Atlantic Multidecadal Variability and Associated Climate Impacts, *Reviews of Geophysics*, [Crossref](#)

Corresponding author:

T. V. Belonenko, Saint Petersburg State University, 7–9, Universitetskaya nab., St. Petersburg 199034, Russia. (t.v.belonenko@spbu.ru)